Intergranular Attack of Steel by Molten Copper

Depending on the composition and crystal structure of steel being surfaced with copper, stresses resulting from surfacing under a welding arc together with Cu penetration of steel grain boundaries can result in open cracks of significant size under the Cu deposit

BY W. F. SAVAGE, E. F. NIPPES AND R. P. STANTON

ABSTRACT. Grain-boundary penetration of steel by copper-base alloys is known to occur during brazing operations. The same property which makes the use of Cu-base alloys feasible for filling the narrow capillary gaps used in brazing causes the penetration of steel grain boundaries by Cu. This penetration during brazing normally is of little concern, because no open gaps or cracks occur in the base metal. However, during the surfacing of steel by Cu using a welding arc, stresses are present which exaggerate the condition. As a result, surfacing produces open cracks of significant size beneath the deposit.

Certain steels have greater resistance to penetration because of their composition and crystal structure. This resistance is particularly evident during furnace brazing, where the ability of a steel to restrict Cu penetration can be measured by the depth of penetrating arms and the dihedral angles which are formed. Alloy steels such as 4340, 4140, and Type 304 stainless steel proved to be extremely susceptible to Cu penetration. Alloy and plain-carbon steels, such as 1340, 1050, Armco iron, and carburized Armco iron, had penetration depths less than ⅓ that of the steels previously mentioned, as well as greater dihedral angles. A high-alloy ferritic stainless steel (grade Type 430) was almost completely immune to Cu penetration.

In order to duplicate the conditions which occur during the surfacing process, a fixture was devised which would stress steel samples while a GMA deposit of Cu was made upon them. The results of subsequent tensile tests indicate that the loss of strength and ductility is serious, particularly for steels requiring heat treatment for maximum properties. For example, after quenching and tempering a specimen of 4140 surfaced with Cu with a prestress of 16 ksi, a 53% loss in tensile strength and a 90% loss in % elongation were noted, when compared to the similarly heat-treated base metal.

Introduction

During the process of depositing a Cu-base alloy on a steel substrate by means of a gas metal arc (GMA) process, grain-boundary penetration and cracking frequently occur. This study examines the causes of such cracking, the relative susceptibility of different steels, and the effect of grain-boundary penetration on mechanical properties during this weld-surfacing process.

The application, which was of particular concern, involved depositing a Cu or gilding metal surfacing deposit on an artillery projectile. With this process which was developed during the early 1950's, the deposits are machined and act as rotating bands for artillery projectiles. The primary function of the rotating band is to engage the rifling in a barrel and impart a high rate of spin to the projectile. The spin stabilizes the shell in flight in a manner which is analogous to the stabilization achieved in arrows and rockets by their fins. A second function of the rotating band is to allow the build up of gas pressure behind the projectile in the barrel.

Originally, rotating bands were applied by swaging a ring of metal into a prepared seat in the shell wall. However, it was found that welding had several advantages and could be substituted readily for the swaging process. The first shells surfaced by welding were manufactured from plain C steels such as 1050 and 1030. Because these steels were not adequate for improved designs in artillery ammunition, the use of oil-hardening steels, such as 4140 and 4340, became necessary.

It was the introduction of new shell designs which first prompted a study of copper-steel interface phenomena. Copper penetration of steel grain boundaries during brazing is a common occurrence, but the penetration during welding is more severe. Since all projectiles are examined for cracking using commercial magnetic particle inspection, Cu penetration was seen as cracking. Copper is diamagnetic and, therefore, gives the same indication as an open void. Furthermore, it seemed certain that the new shell steels such as 4140 and 4340 would be more susceptible to penetra-

W. F. SAVAGE is Professor of Metallurgical Engineering and Director of Welding Research, and E. F. NIPPES is Professor of Metallurgical Engineering, Rensselaer Polytechnic Institute, Troy, N. Y.; R. P. STANTON, former Graduate Assistant at RPI, is now with the Department of the Army, Frankford Arsenal, Philadelphia, Pennsylvania.

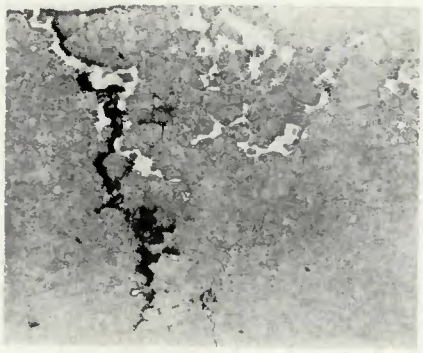

Fig. 1—Open and Cu-filled cracks in 4340 steel which has been GMA surfaced with Cu. Nital etch, ×250 (reduced 50% during printing reproduction)

Fig. 2—Cracks at the surface of 4340 steel which has been GMA surfaced with Cu. Cu surfacing deposit has been chemically removed and center position has been machined. ×2 (reduced 50% during printing reproduction)

tion than 1030 or 1050 had been.

During the weld-surfacing process, a Cu wire is fed as the electrode of a DCRP inert-gas-shielded welding arc. A second Cu wire is fed into the arc, when established, to add additional metal and reduce the intensity of the arc plasma which touches the steel. The projectile is rotated and the torch oscillated to produce the size of surfacing deposit desired.

Historical Review

Numerous researchers within the Soviet Union have reported wide variations in susceptibility of steel to grain-boundary penetration by Cu-base alloys. Asnis and Prokhorenko[1] found that Cu would not wet a ferritic steel, whereas a pearlitic steel was readily wet. They recognized that the cracks which form during the surfacing process are initiated by the same wetting process which occurs during the brazing of steel.

Bredzes and Schwartzbart[2] contributed a great deal of knowledge concerning the propensity of Cu to penetrate steel grain boundaries during brazing. They reported that, in low-C steel, penetration does not occur immediately and must await diffusion of C to grain boundaries. They also reported observing no delay in Cu penetration of eutectoid steels.

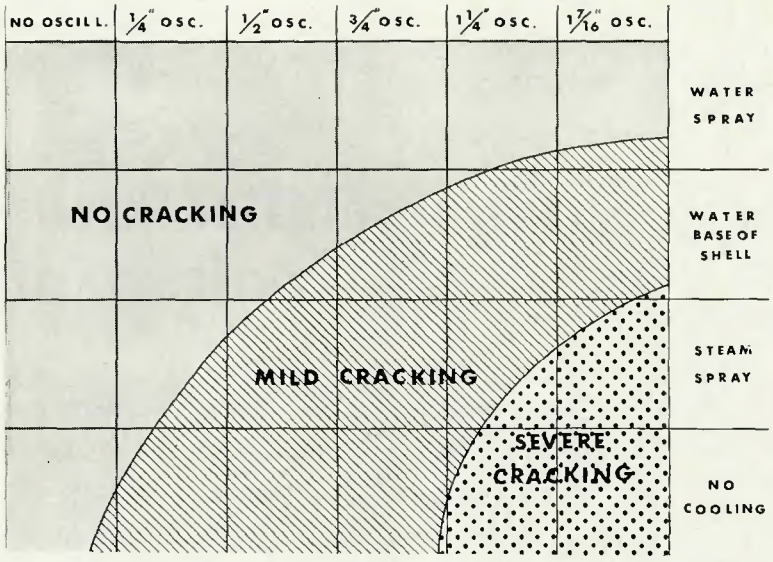

Fig. 3—Cracking tendency as a function of oscillation and shell-cooling practice

It is completely plausible for C to diffuse against a concentration gradient, i.e., from homogeneous distribution within the grain to high concentration at grain boundaries.[3] Bredzes further concluded that in alloy steels penetration is controlled by how those elements, which are present, influence the ability of C to seek out Cu-enriched grain boundaries.

Bozhko[4] developed an equation for the penetration of steel by immersion in molten Cu:

$$X^2 = 4Dt$$

where X = depth of penetration, t = time, and D = diffusion coefficient, i.e.,

$$D = D_o e^{-\frac{Q}{RT}}$$

His most significant conclusion, which would seem to corroborate the experimental findings of Bredzes, stated, "the activation energy for the boundary diffusion of molten Cu into steel depends on the composition of the steel; the higher the C content of the steel, the lower the activation energy."

It is evident from the rate equation that both the temperature of the molten Cu and the time it remains molten are important determinants of penetration depth. These facts would seem completely logical and have offered the most easily regulated variables in the reduction or elimination of cracking.

Figure 1 illustrates, in a section perpendicular to Cu surfaced on 4340 steel, numerous voids and Cu-filled cracks. Considerable penetration of Cu into prior austenitic grain boundaries has occurred. Because of the stress associated with the surfacing process, some areas are not completely filled with Cu; these are open voids.

It is possible to remove a Cu band completely by a chemical etching technique without damage to underlying steel. An example of this Cu removal is presented in Fig. 2 which shows the surfaced area from which the center portion was machined to disclose the depth of the cracks formed. Notice that the greatest amount of cracking occurs in the area of greatest melting of the steel.

When cracking was first recognized in the application of Cu to 4000 series steels, a quick empirical study was made to find a way of eliminating or reducing the problem. Figure 3 demonstrates the influence that surface deposit size and different types of cooling on the shell wall have in reducing cracking. As a result, surfacing deposit widths were reduced and application of water spray beneath the puddle was utilized as a standard procedure. By such means, the time available for molten Cu to penetrate stressed austenite grain boundaries was reduced.

Valermann and Osetnik[5] in their experiments compared crack frequency with types of application technique. Using a plasma arc, the authors were able to reduce greatly the cracking which had been experienced during submerged-arc surfacing. Thus, in addition to reducing the length of time available for penetration to occur, the plasma arc apparently reduces the stress level by limiting the size of the heat-affected zone. A discussion of the source of stress in the surfacing process follows.

Theory

Intergranular penetration and cracking are related to the ability of a liquid

metal to "wet" metals in the solid state. As mentioned previously, empirical observations have shown a greater ease for Cu to penetrate austenite boundaries of certain grades of steel. Experimental evidence of such observations, in the form of photomicrographs, is presented later.

The term "wetting" has been defined as: "A phenomenon involving a solid and a liquid in such intimate contact that the adhesive force between the two phases is greater than the cohesive force within the liquid."[6] Intergranular penetration, which may be thought of as a special example of spreading of a fluid within a grain boundary, represents an incoherent boundary between two phases. Smith[7] explains that the surface energies of the boundaries play an important role in determining the shape of the penetrating phase. Figure 4 shows schematically the type of structure which is formed in cases where a second phase β is located at the junction of three grains of the main phase α. After equilibration at temperatures above the melting point of phase β, the shape of this included phase becomes adjusted to minimize the surface energy of the system.

A balance of the surface tension forces determines the phase shape; these forces at the junction of the grain boundary (OC) and the two interphase boundaries (OA) and (OB) are shown in Fig. 4. If the surface free energies are denoted by $\gamma_{\alpha\alpha}$ and $\gamma_{\alpha\beta}$ respectively, then θ is given by the relation:[7]

$$\gamma_{\alpha\alpha} = 2\,\gamma_{\alpha\beta}\cos\frac{\theta}{2}$$

If $2\,\gamma_{\alpha\beta} < \gamma_{\alpha\alpha}$, the dihedral angle is 0 deg, and the second phase will spread as a continuous film. Hot shortness of steel is caused by the spread of various low-melting-point liquids (sulfides) by this mechanism.[8]

The values of $\gamma_{\alpha\alpha}$ and $\gamma_{\alpha\beta}$ are difficult to determine. In the case of molten Cu and solid Fe, one source[9] has experimentally determined $\gamma_{Fe\text{-}Fe}$ as 850 ergs/cm^2 and $2\gamma_{Fe\text{-}Cu}$ as 860 ergs/cm^2 at 2021 F (1105 C). These values predict a dihedral angle of approximately 18 deg.

Thus far, the discussion has concerned the factors which influence grain-boundary penetration when the substrate steel is fully heated to the temperature of the molten Cu. During the surfacing of Cu on shell bodies, only a small portion of the wall thickness becomes austenitic. When ferrite transforms to austenite, a volume contraction occurs. However, because this contraction is restrained by the underlying ferrite, a tensile stress is applied to the steel directly beneath the molten Cu. This stress, in the presence of a liquid metal which has great affinity to penetrate austenite grain boundaries, produces the cracks seen in Fig. 1. Thus, the process of applying Cu surfacing deposits to steel is a distinct example of liquid-metal embrittlement.

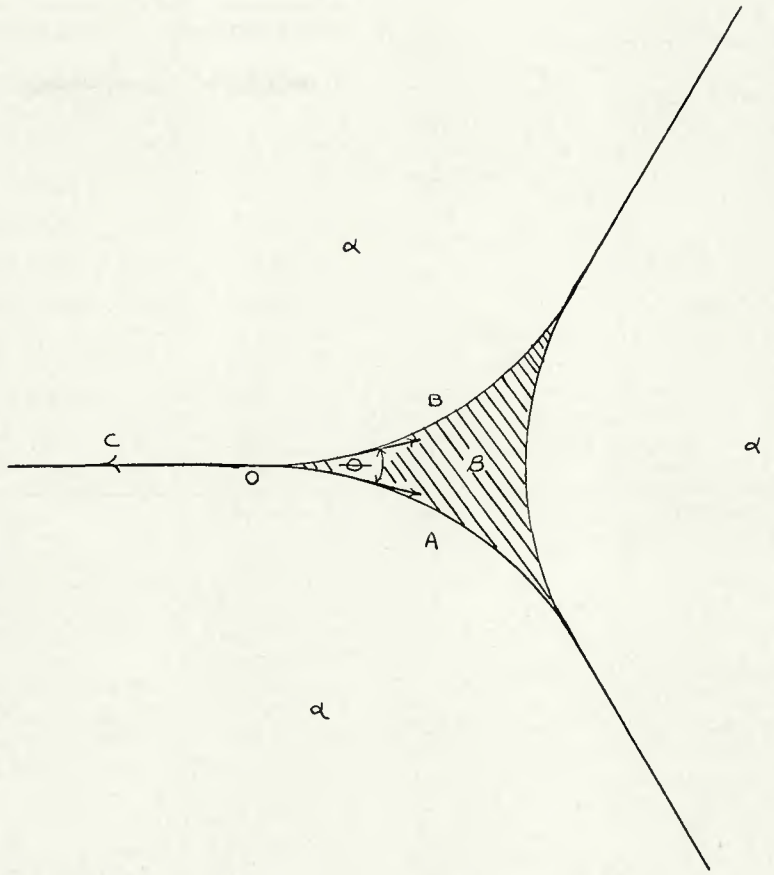

Fig. 4—Schematic of the location of a second phase β at the intersection of 3 grains of the primary phase α

Eborall and Gregory,[10] in their paper on embrittlement by a liquid phase, have compared surface-energy requirements to form a crack with and without a liquid present.

With transgranular cracking, the total energy required to form a crack is equal to the total area of the newly formed surface (two times the surface area of one side of the crack) multiplied by the surface free energy per unit area, γ_s. Thus, the energy per unit area E_T is equal to $2\gamma_s$.

In the case of grain-boundary cracking, the surface free energy of the grain boundary $\gamma_{\alpha\alpha}$ must be subtracted from the surface free energy of the newly formed surface $2\gamma_s$. Thus, the energy per unit area E_G is equal to $2\gamma_s$-$\gamma_{\alpha\alpha}$.

In the case of grain-boundary penetration by a liquid, the surface free energy term γ_s must be replaced with the solid-liquid free energy $\gamma_{\alpha\beta}$. Thus, the energy per unit area E_p is equal to $2\gamma_{\alpha\beta}$-$\gamma_{\alpha\alpha}$.

From energy determinations made in the Cu-Bi system, Eborall *et al*[10] found that the energy required to propagate a grain-boundary crack is some 15 times less if a liquid is present. Eborall *et al* determined the variation of cracking energy E with dihedral angle, as follows:

$$E = 2\gamma_{\alpha\beta} - \gamma_{\alpha\alpha}$$

but since, $\gamma_{\alpha\alpha} = 2\gamma_{\alpha\beta}\cos\frac{\theta}{2}$

(see Smith[7])

$$\text{therefore, } E = \gamma_{\alpha\alpha}\left(\sec\frac{\theta}{2} - 1\right)$$

The experimenters concluded that, because the energy to form a crack does not change drastically at small angles ($\theta < 30$ deg), differences in dihedral angle should not be used as crack-sensitivity criteria. However, the Griffith theory states that the stress to form a crack is proportional to the square root of the energy to form a new surface. If this is the case, the stress required to propagate a crack would be a much more sensitive indicator of cracking sensitivity. Experimental results of this research program will corroborate that, given sufficient stress, cracking proceeds rapidly regardless of dihedral angle measured in unstressed specimens. However, differences in cracking sensitivity have been detected during actual welding operations where no augmented stress

had been applied.

Stoloff[11] does not believe that use of surface energies determined from wetting experiments can be used quantitatively to measure crack-propagation energy. In his work, an equation is presented for the stress σ to propagate a crack:

$$\sigma = \frac{E_o \gamma_o p}{4 a_o c}$$

where

E_o = Young's modulus
γ_o = Surface energy
a_o = Interatomic spacing
p = Crack radius
c = Crack length

Plastic deformation increases the effective crack radius and this in turn alters the surface energy term such that:

$$\gamma_{eff} = \frac{\gamma_o p}{a_o}$$

Stoloff explains that the presence of a liquid will reduce γ_o; this was demonstrated in the studies of Eborall and Gregory.[10] Although not calculated quantitatively, it is frequently determined experimentally that the cohesive stress is reduced by liquids. Reduction of the cohesive stress prevents shear stress from blunting the crack tip. Thus, the liquid-filled discontinuity is always a sharp crack. It is further stipulated that for crack-insensitive materials, i.e., those with FCC lattice, liquid must always be present at the crack tip to allow the crack to propagate at a reduced stress. It is known that Cu can easily fill a narrow capillary gap, such as a grain-boundary crack in steel.

Experimental Procedures

In the first stage of this study, Cu was furnace-melted on steel tabs to determine differences in Cu penetration. The steel tabs, 2 in. (51 mm) square × ¼ in. (6.4 mm) thick, were wrapped with Cu welding wire, placed on alundum grain, and heated in a dry H_2 atmosphere (cracked NH_3) for 2 h at 2050 F (1121 C). The welding wire, originally developed by Cyril Stanley Smith, has improved wetting characteristics over that of pure Cu. Wire composition and the composition of steel alloys used in the study are given in Table 1. Each tab was sectioned and examined metallographically.

Because a furnace environment does not develop the stresses associated with the surfacing process, a fixture was designed which would allow the application of selected loads to standard ASTM flat tensile specimens during the surfacing process. The fixture consists of a three-point loaded beam with one end supported by the tensile specimen, and the other by a force gage. A screw adjustment was provided to ensure a balanced load. The motive force is supplied by a 20 ton (18 metric ton) hydraulic hand jack. The arc is initiated on a tab and travels transversely across the tensile specimen as illustrated in Fig. 5. A 0.045 in. (1.14 mm) diameter Cu electrode was used with a 0.0625 in. (1.6 mm) diameter auxiliary or "cold" (i.e., electrically neutral) Cu wire. The larger "cold" wire prevents excessive melting of the steel. The energy input of 33 kJ/in. (13 kJ/cm) was selected so that transformation to austenite occurred throughout the transverse cross section of the tensile specimen.

The GMA welding conditions were as follows: shielding gas—argon; current—185 to 190 A; voltage—20 to 21 V; travel speed—7 ipm (2.96 mm/sec).

To check the accuracy of the load-measuring system, a tensile specimen with an attached strain gage was loaded in a calibrated tensile machine and then in the fixture. The results showed acceptable accuracy for the load-measuring system.

Each of a series of tensile specimens was preloaded and Cu surfaced in the fixture. The specimens were then heat treated, either by annealing or by quenching followed by tempering for 1 h at 1000 F (538 C). Tensile tests were conducted on the specimens after heat treatment.

Table 1—Composition of Steel Substrates Used in Study of Penetration, %

Steel	C	Mn	P	5	Si	Ni	Cr	Mo
4140	0.40	0.83	0.012	0.009	0.26	0.11	0.94	0.21
4340	0.40	0.68	0.020	0.013	0.28	1.87	0.74	0.25
1340	0.40	1.77	0.027	0.016	0.25	0.10	0.12	0.01
1050	0.54	0.69	0.012	0.030	0.19	–	–	–
1026	0.25	0.75	0.040	0.050	–	–	–	–
Armco iron	0.025	0.045	0.005	0.015	–	–	–	–
304 stainless	<0.08	<2.00	–	–	<1.00	10	19	–
430 stainless	<0.12	<1.00	–	–	<1.00	<0.50	16	–

Composition of Copper Electrode, %

Cu	Pb	Fe	Zn	Sn	Bi	Ni	Sb	Al	Mn	As	P	Ag	5i
98.82	ND[a]	0.03	ND	0.63	ND	0.005	ND	ND	0.35	ND	ND	0.005	0.14

[a]Not detectable

Results and Discussion

Furnace Brazing Studies

Figures 6 and 7 illustrate the influence of C content on Cu penetration; Fig. 6 shows a photomicrograph of Armco iron, and Fig. 7 shows carburized Armco iron with approximately 0.8% C. The depth of penetration in

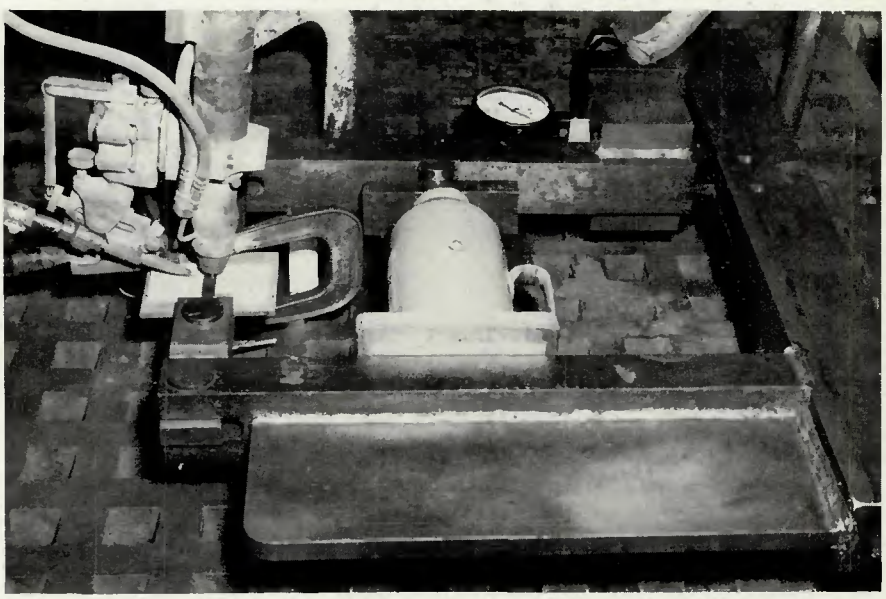

Fig. 5—Location of the tensile specimen in the fixture for applying stress during the Cu surfacing process

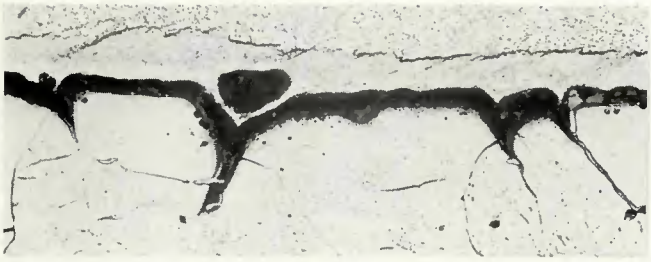

Fig. 6—Photomicrograph of Armco iron after furnace-brazing exposure to Cu for 2 h at 2050 F. Nital etch, ×500 (reduced 47% during printing reproduction)

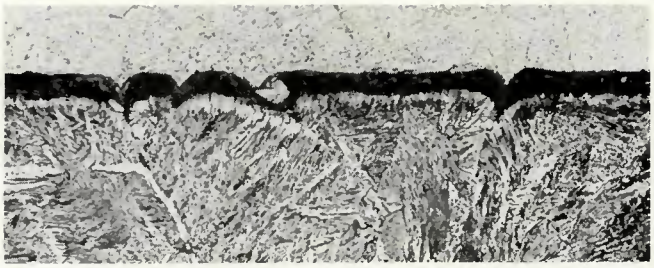

Fig. 7—Photomicrograph of carburized Armco iron after furnace-brazing exposure to Cu for 2 h at 2050 F. Nital etch, ×500 (reduced 47% during printing reproduction)

Fig. 8—Photomicrograph of decarburized 4340 steel after furnace-brazing exposure to Cu for 2 h at 2050 F. Nital etch, ×500 (reduced 59% during printing reproduction)

Fig. 9—Photomicrograph of 1026 steel after furnace-brazing exposure to Cu for 2 h at 2050 F. Nital etch, ×500 (reduced 50% during printing reproduction)

Fig. 10—Photomicrograph of Type 304 stainless steel after furnace-brazing exposure to Cu for 2 h at 2050 F. As polished, ×500 (reduced 50% during printing reproduction)

both samples is low, and the dihedral angle is quite large. Thus, the C content did not exert as strong an influence on penetration kinetics as Bredzes and Schwartzbart predicted.[2] It is apparent that considerable diffusion of Cu into iron has occurred, which has complicated the interpretation of these photomicrographs.

Fig. 11—Photomicrograph of Type 430 stainless steel after furnace-brazing exposure to Cu for 2 h at 2050 F. Vilella's etch, ×500 (reduced 50% during printing reproduction)

The relatively minor effect of C content on Cu penetration was also noted when 4340 and 4140 steels were compared both in the as-received and decarburized conditions. The large depth of penetration and the relatively sharp dihedral angles, shown in Fig. 8 for decarburized 4340 steel, are typical of those found in as-received and decarburized 4140 and 4340. In Fig. 8, it appears that the residual C, remaining after decarburization, has diffused toward the Cu-penetration arms.

Figure 9 illustrates the significant depth of Cu penetration and the dihedral angle for 1026 steel. It appears that C has diffused away from Cu in this steel. In one prior-austenitic grain, completely surrounded by Cu, the C has been forced to the center of the grain, forming a pearlitic colony.

Both 1340 and 1050 steels, similar to the Armco irons, showed only a small amount of Cu penetration during the furnace-brazing tests. As previously discussed, it was the replacement of 1050 by 4140 which first demonstrated the need to investigate the Cu-penetration phenomena.

Figures 10 and 11 illustrate two high-alloy steels of special characteristics. Type 304 stainless steel, shown in Fig. 10, is austenitic (FCC) at all temperatures. The depth of penetration and

Fig. 12—Cracks in a 4340 steel specimen which has been GMA surfaced with Cu while under a 16 ksi stress. Cu has been chemically removed. 2× (reduced 50% to original size during printing reproduction)

dihedral angles are of the same magnitude as those found for 4140 and 4340 steels. Because of the mutual solid solubility of Ni and Cu, extensive intermixing of the steel and Cu occurs in the system. In some cases, it was impossible to identify the original interface, as will be noted in Fig. 10.

The character of the microstructure illustrated in Fig. 11 for Type 430 stainless steel is in sharp contrast with previous examples. In this case, the minor depth of penetration and the large dihedral angle (approximately 100 deg) are indicative of a material which would not be affected by Cu surfacing. The influence of surface free

energy on the ability of a liquid phase to wet grain boundaries has been discussed previously. With this steel, the matrix remains ferritic (BCC) even at 2050 F (1121 C). Contrast this with Type 304 stainless steel which, because of the high-Ni content, has high mutual solubility with Cu and whose grain boundaries are easily wet by molten Cu.

Russian investigators[4] have reported behavior identical to that of Type 430 steel when Cu surfacing deposits were deposited on high-Si transformer steel. These steels are also ferritic (BCC) at the melting point of Cu.

Table 2—Effect of Prestress During Cu Surfacing on Mechanical Properties of Armco Iron and Carburized Armco Iron, Annealed after Surfacing

Alloy	Prestress ksi[a]	Yield strength, ksi[a]	Tensile strength, ksi[a]	Elongation in 2 in., %
Armco iron	Annealed only	18.2	38.0	45.5
Armco iron	0	15.0	37.4	21.0
Armco iron	8	15.5	36.5	18.0
Armco iron	8	16.4	35.2	15.0
Armco iron	16	17.1	24.2	6.6
Armco iron	25	18.9	25.3	6.0
Armco iron	25	18.3	35.9[b]	9.1
0.8%C Armco	Annealed only	38.8	77.9	16.2
0.8%C Armco	0	23.3	58.3	26.2
0.8%C Armco	12	23.5	52.4	9.1
0.8%C Armco	16	23.3	30.5	3.8
0.8%C Armco	16	24.2	63.2	5.0
0.8%C Armco	20	25.5	37.2	3.8

[a]Multiply ksi by 6.895 to obtain MPa.
[b]Cu penetrated entire section.

Table 3—Effect of Prestress During Cu Surfacing on Mechanical Properties of 4140 and 4340 Steels Annealed after Surfacing

Alloy	Prestress, ksi[a]	Yield strength, ksi[a]	Tensile strength, ksi[a]	Elongation in 2 in., %
4140	Annealed only	51.1	100.1	24.4
4140	0	50.4	92.0	24.0
4140	10	50.8	94.7	22.4
4140	16	48.3	88.9	11.0
4140	24	49.2	78.3	7.0
4140	24	28.9	28.9	1.6
4140	32	51.0	76.4	6.0
4340	Annealed only	77.3	133.6	16.0
4340	16	66.5	96.8	5.0
4340	24	61.0	70.4	3.0

[a]Multiply ksi by 6.895 to obtain MPa.

Table 4—Effect of Prestress During Cu Surfacing on Mechanical Properties of Types 304 and 430 Stainless Steels Annealed after Surfacing

Alloy	Prestress, ksi[a]	Yield strength, ksi[a]	Tensile strength, ksi[a]	Elongation in 2 in., %
304	Annealed only	29.2	84.1	73.0
304	0	26.9	55.8[b]	19.6
304	0	27.4	70.0	35.8
304	14.6	25.3	58.9	25.0
304	22.6	21.3	45.9	12.7
430	Annealed only	45.2	72.8	26.0
430	2.3	51.1	79.0	18.0
430	34	57.0	84.9	12.0
430	34	48.4	73.8	11.8

[a]Multiply ksi by 6.895 to obtain MPa.
[b]Considerable intergranular penetration.

Prestressed Specimen Studies

The magnitude of the cracking problem was significantly greater when stress was applied using the weld test fixture during the Cu-surfacing process. As an example, Fig. 12 shows the cracks which were revealed in a prestressed tensile specimen of 4340 steel after most of the Cu surfacing deposit had been removed chemically.

Tables 2–5 outline the results of tensile tests performed on steel specimens which had been prestressed during the surfacing process. Some specimens were surfaced without prestressing, while others were tensile tested without Cu surfacing, as a check on base-metal properties. The majority of specimens were annealed after surfacing; these results are presented in Tables 2–4. Three groups of specimens were also quenched-and-tempered after surfacing; these results are given in Table 5. The results of this prestressing study are summarized below.

It was found that all steels, with the exception of Type 430 stainless, developed cracks when sufficient prestress was applied. Furthermore, all steels which did crack had done so at a prestress level less than 16 ksi (110 MPa). Figures 13 and 14 show the variation in the tensile strength, yield strength, and % elongation between annealed base-metal properties and those of tensile specimens which were surfaced with a prestress of 16 ksi (110 MPa) and annealed after welding. There are significant reductions in the values of the elongation and tensile strength. However, the yield strength, which is of primary importance in structural designs, was not reduced substantially.

The probable explanation for the retention of yield-strength properties can be understood by the observation that (in brazed joints) as the width of the capillary gap is reduced, the properties approach those of the base metal. Thus, the complete filling of a grain boundary would certainly be analogous to a narrow capillary gap found in brazing. One sample of Armco iron was penetrated through its entire cross section by Cu during surfacing. The resultant mechanical properties of this sample following annealing were better than those of a similar specimen which had not been completely penetrated—Table 2.

It had been hoped that the threshold level of stress, at which a particular steel began cracking, could be determined. However, it became evident that the test procedure, which was capable of providing increments of prestress as small as 4 ksi (27.6 MPa), was not sufficiently sensitive to detect

Fig. 13—Mechanical properties of Type 304 and 430 stainless steels and Armco iron before and after GMA surfacing with Cu with a prestress of 16 ksi. Annealed conditions

that level. In general, however, the greater the prestress, the greater was the loss in tensile strength and % elongation for a given steel. The loss in yield strength was much more gradual; in one case (carburized Armco iron), the yield increased slightly with increasing level of prestressing.

A much greater resistance to cracking was exhibited by Type 430 stainless, a steel poorly wet by Cu during furnace studies, than by 4340, which experienced considerable penetration and sharp dihedral angles. When both steels were prestressed to 40 ksi (275.8 MPa) prior to surfacing, absolutely no cracking occurred in Type 430 stainless steel, whereas considerable cracking occurred in the 4340, as shown previously in Fig. 12.

In systems where liquid-metal embrittlement is caused by intergranular penetration, the wetting behavior of the liquid can be more important than the level of prestressing. For example, two specimens of Type 304 stainless were surfaced without prestressing—Table 4. One of these specimens was severely penetrated by Cu and suffered a 73% loss in elongation and a 34% loss in tensile strength. The other specimen was less severely penetrated, and suffered a 51% loss in elongation and a 17% loss in tensile strength. Because of the great affinity for Cu to wet the grain boundaries of this steel, severe loss of properties can occur even without augmented stress.

Significant loss of mechanical properties occurred when 4140, 4340, and 0.8% C Armco iron were quenched-and-tempered after surfacing—Table 5. Both 4340 and 4140 behaved in such a brittle manner that a yield strength value could not be determined. Table 6 compares the % loss in tensile strength and the % loss in % elongation for samples which were Cu-surfaced with a prestress, and were either annealed or quenched-and-tempered after surfacing. The % loss was calculated using the appropriate mechanical properties of the base metal which had been either annealed or quenched-and-tempered without being subjected to the surfacing process.

As may be noted from Table 5 and Fig. 15, specimens that are quenched-and-tempered to bring out the highest

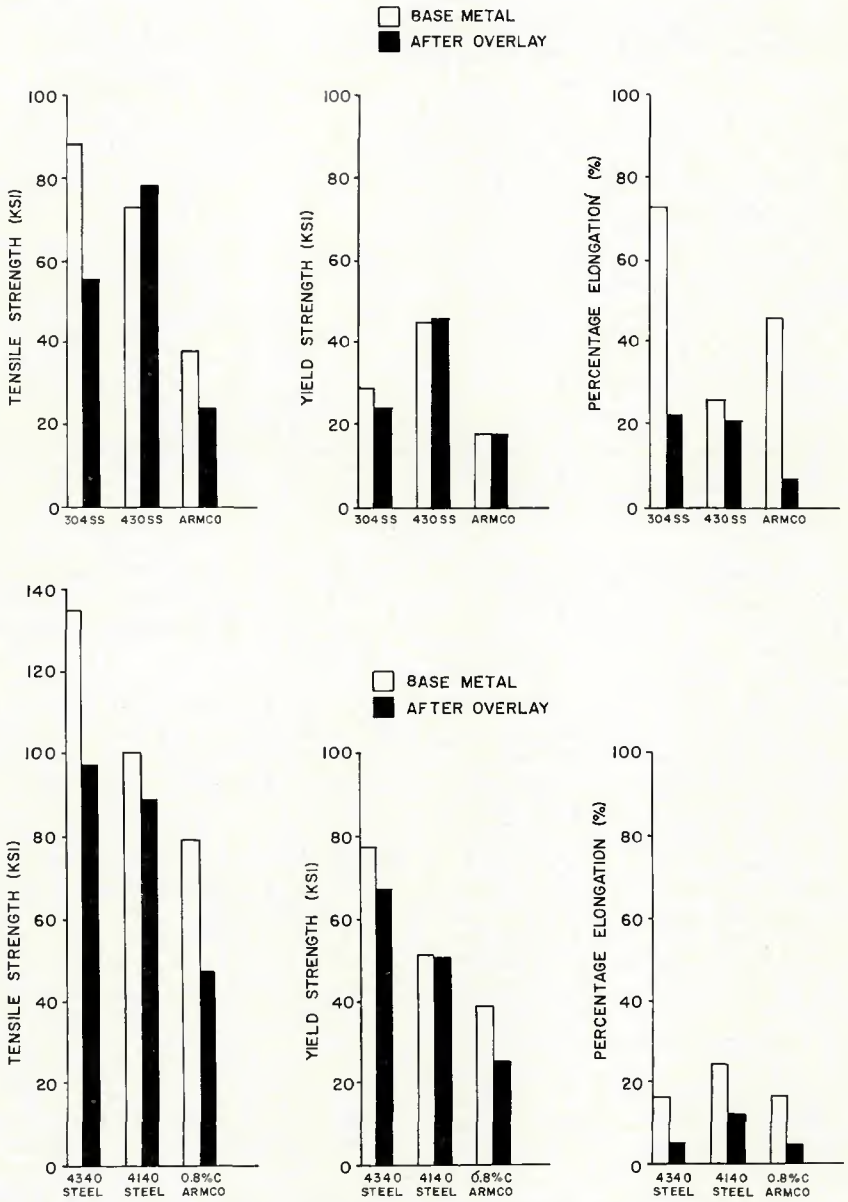

Fig. 14—Mechanical properties of 4340 and 4140 steels and carburized Armco iron before and after GMA surfacing with Cu with a prestress of 16 ksi. Annealed conditions

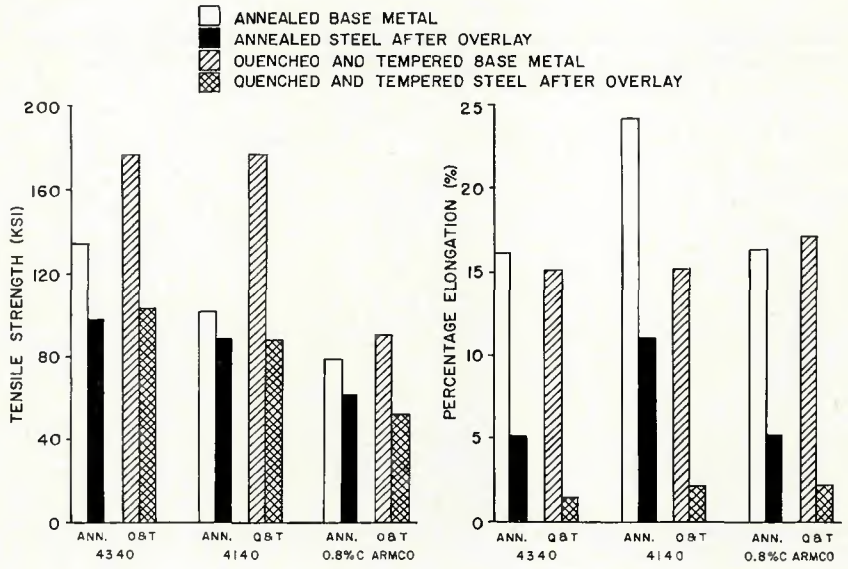

Fig. 15—Mechanical properties of 4340 and 4140 steels and carburized Armco iron before and after GMA surfacing with Cu with a prestress of 16 ksi. Both annealed and quenched-and-tempered conditions

Table 5—Effect of Prestress During Cu Surfacing on Mechanical Properties of 4140 and 4340 Steels, and Carburized Armco Iron, Quenched-and-Tempered after Surfacing

Alloy	Prestress, ksi[a]	Yield strength, ksi[a]	Tensile strength, ksi[a]	Elongation in 2 in., %
4140	Quenched-and-tempered only	150.0	167.0	15.0
4140	16	[b]	88.0	1.6
4140	24	[b]	56.9	0.8
4340	Quenched-and-tempered only	165.9	174.7	15.2
4340	16	[b]	101.9	1.5
0.8%C Armco	Quenched-and-tempered only	65.4	90.0	16.6
0.8%C Armco	16	50.0	50.4	1.6

[a]Multiply ksi by 6.895 to obtain MPa.
[b]Material too brittle for yield-strength determination.

potential properties of the heat-treatable steel are most severely affected by the presence of open cracks. Note also, as shown for 4140, that the loss in mechanical properties is greater for higher values of prestress levels.

It is obvious that steels become more notch sensitive when quenched-and-tempered to high-strength levels. In the presence of cracks partially filled with Cu, of the type shown in Fig. 1, the mechanical properties are adversely affected. Cracks of this type will propagate during tensile testing in a brittle fashion in a steel which has been heat treated to high-strength levels and, as a result, has become notch sensitive. Finally, the results agree with those of Rostocker *et al*[12] who found that for a given alloy composition, high-strength alloys were more severely embrittled by liquid metals than were low-strength alloys.

Conclusions

1. When stresses are not present, the ease with which a molten Cu alloy will penetrate steel grain boundaries is determined by the composition of the steel.

2. The ease of grain-boundary penetration by Cu into a steel can be measured by the penetration depth and the dihedral angle. A smaller dihedral angle signals a greater ease of penetration.

3. Of those alloying elements commonly found in steel, C exerts the least influence on penetration depth and dihedral angle.

4. For a steel undergoing Cu surfacing, the stress required to initiate a crack is reduced substantially if the austenitic grain boundaries are wet by Cu.

5. When grain-boundary penetration occurs, stress application during the surfacing process results in partially-filled or open cracks in the steel.

6. Because solid Cu in a grain boundary is analogous to a braze in a narrow capillary gap, the mechanical properties of a steel which is in the annealed condition are not greatly impaired after Cu surfacing.

7. Notch-sensitive heat-treated steels lose much of their strength and ductility when partially filled Cu cracks are present.

8. Steels which remain ferritic at the melting point of Cu will not lose strength as a result of exposure to molten Cu.

9. Common steels could not be segregated on the basis of resistance to intergranular cracking when artificial stress was applied. However, resistance was detected during furnace-melting studies and frequent empirical observations during magnetic-particle inspection of welded surfacing rotating bands.

Table 6—Effect of Cu Surfacing on the Loss in Postheat-Treated Mechanical Properties

Alloy	Prestress during surfacing, ksi[a]	Postheat Treatment	Loss in Tensile Strength, %	Loss in Elongation, %
0.8%C Armco	16	annealed	19	69
0.8%C Armco	16	quench & temp.	44	90
4140	16	annealed	11	55
4140	16	quench & temp.	53	90
4140	24	annealed	22	71
4140	24	quench & temp.	66	95
4340	16	annealed	28	69
4340	16	quench & temp.	42	90

[a]Multiply ksi by 6.895 to obtain MPa.

Acknowledgment

This paper is based upon a thesis submitted in partial fulfillment of the requirements for a Master of Materials Engineering degree. The work was funded by the United States Government and conducted at Frankford Arsenal. The authors wish to acknowledge the interest and support of Mr. Irving Betz, Chief, Materials Processing Branch, and the efforts of Mr. Richard Schlauch, who performed the welding operations.

References

1. Asnis, E. A., and Prokhorenko, V. M., "Mechanism of Cracking During the Welding or Depositing of Copper onto Steel," *Svar. Proiz.*, No. 11, (1965), pp. 8-9.

2. Bredzes, N., and Schwartzbart, "Fundamentals of Brazing," Report to Frankford Arsenal (1956).

3. Darken, S. L., "Diffusion of Carbon in Austenite with a Discontinuity of Composition," *Transactions*, AIME, Vol. 180, (1949) pp. 430-438.

4. Bozhko, A. M., "Mechanism by Which Molten Copper Penetrates into Steel," *Art Svarka*, No. 7, (1968), pp. 25-28.

5. Vaierman, A. E., and Osatnik, A. A., "The Formation of Cracks During the Deposition of Copper Alloys on Steel," *Art Svarka*, No. 6, (1968), pp. 23-25.

6. A.S.M., *"Metals Handbook,"* Vol. 1, ASM, Metals Park, Ohio, (1961), p. 41.

7. Smith, C. S., "Grains, Phases and Interfaces: An Interpretation of Microstructure," *Transactions*, AIME No. 175 (1948) pp. 15-48.

8. Cottrell, A. H., *Theoretical Structural Metallurgy*, St. Martin's Press Ind., N. Y., N. Y., (1955), 150-151.

9. Van Vlack, L. R., "Intergranular Energy of Iron and Some Iron Alloys," *Transactions*, AIME, 191, (1951), pp. 231-259.

10. Eborall, R., and Gregory, P., "The Mechanism of Embrittlement by Liquid Phase," *J. Inst. Met.*, 84, (1955), pp. 88-90.

11. Stoloff, N. S., "Liquid Metal Embrittlement," *Surfaces and Interfaces*, Vol. 11, (1968), pp. 157-181.

12. Rostoker, W., McCaughey, J. M., and Markus, H., *Embrittlement by Liquid Metals*, Reinhold Publishing Corp., N. Y., N. Y., (1960) pp. 61-62.